MicroRNA-130a-3p inhibition suppresses cervical cancer cell progression

RHAFAELA LIMA CAUSIN[1], ANDRÉ VAN HELVOORT LENGERT[1], IZABELA NATALIA FARIA GOMES[1], ANA JULIA AGUIAR DE FREITAS[1], MARCELA NUNES ROSA[1], RICARDO DOS REIS[2], RUI MANUEL REIS[1,3,4] and MÁRCIA MARIA CHIQUITELLI MARQUES[1]

[1]Molecular Oncology Research Center, Barretos Cancer Hospital, Teaching and Research Institute; [2]Department of Gynecological Oncology, Barretos Cancer Hospital, Barretos, São Paulo 14784-400, Brazil; [3]Life and Health Sciences Research Institute (ICVS/3B's)-Government Associate Laboratory, 4806-909 Braga; [4]Life and Health Sciences Research Institute, Medical School, University of Minho, 4704-553 Braga, Portugal

Received November 3, 2022; Accepted February 17, 2023

DOI: 10.3892/or.2023.8546

Abstract. MicroRNAs (miRNAs or miRs) play essential roles in the initiation and progression of human tumors, including cervical cancer. However, the mechanisms underlying their actions in cervical cancer remain unclear. The present study aimed to evaluate the functional role of miR-130a-3p in cervical cancer. Cervical cancer cells were transfected with a miRNA inhibitor (anti-miR-130a-3p) and a negative control. Adhesion-independent cell proliferation, migration and invasion were evaluated. The findings presented herein demonstrated that miR-130a-3p was overexpressed in HeLa, SiHa, CaSki, C-4I and HCB-514 cervical cancer cells. The inhibition of miR-130a-3p significantly reduced the proliferation, migration and invasion of cervical cancer cells. The canonical delta-like Notch1 ligand (*DLL1*) was identified as a possible direct target of miR-103a-3p. The *DLL1* gene was further found to be significantly downregulated in cervical cancer tissues. On the whole, the present study demonstrates that miR-130a-3p contributes to the proliferation, migration and invasion of cervical cancer cells. Therefore, miR-130a-3p may be used as a biomarker to determine cervical cancer progression.

Correspondence to: Dr Márcia Maria Chiquitelli Marques, Molecular Oncology Research Center, Barretos Cancer Hospital, Teaching and Research Institute, 1,331 Anternor Duarte Vilela, Barretos, São Paulo 14784-400, Brazil
E-mail: mmcmsilveira@gmail.com

Abbreviations: UTR, untranslated region; CESC, cervical squamous cell carcinoma and endocervical adenocarcinoma; CIN3, cervical intraepithelial neoplasia grade 3; DLL1, delta-like notch 1 ligand; FDR, false discovery rate; HPV, human papillomavirus; LACC, locally advanced cervical cancer; mirDIP, microRNA Data Integration Portal; miRNA/miR, microRNA; RT-qPCR, reverse transcription-quantitative PCR; TCGA, The Cancer Genome Atlas; *WNT10A*, Wnt family member 10a

Key words: cervical cancer, microRNA-130a-3p, biomarker, tumor progression

Introduction

Cervical cancer is the fourth most frequently diagnosed type of cancer and the fourth leading cause of cancer-associated mortality among women, with an estimated 604,000 new cases and 342,000 related mortalities worldwide in 2020 (1). In Brazil, cervical cancer is the third most common type of cancer among women (1). Despite improved prevention programs, numerous patients are diagnosed at a locally advanced stage, and the prognosis and 5-year survival rate of patients with locally advanced cervical cancer (LACC) remain poor (2). The standard treatment for LACC is radiotherapy concomitant with platinum-based chemotherapy (3,4). However, >50% of patients on this treatment regimen may experience resistance to therapy (5).

It is well understood that, although human papillomavirus (HPV) infection is necessary to immortalize cervical cells, this infection is not sufficient to lead to their transformation (6). For this reason, studies have indicated that epigenetic mechanisms may be involved in the process of cervical tumor progression (7). Therefore, it is essential to elucidate the molecular mechanisms underlying the progression of cervical cancer.

Recently, the concept of the non-mutational epigenetic regulation of gene expression was demonstrated as a novel hallmark of cancer (8). There is increasing evidence to indicate that these epigenetic alterations may contribute to tumor development and malignant progression. MicroRNAs (miRNAs or miRs) can modulate the pathophysiological mechanisms of cervical cancer, which may provide novel approaches for the diagnosis and treatment of patients with cervical cancer in the future (9,10). miRNAs are short (~22 nucleotides in length) non-coding RNAs that generally control gene expression at the post-transcriptional level through mRNA degradation or translational repression (11), and have been reported to function as oncomiRs or tumor-suppressor miRNAs (12). miRNAs

can play essential roles in cell proliferation, migration and invasion in cervical cancer (9,13). Therefore, it is necessary to investigate the functional role of previously identified miRNAs that are differentially expressed and associated with a higher odds ratio for the progression of high-grade cervical cancer lesions and, consequently, invasive cervical cancer.

The canonical delta-like Notch1 ligand (*DLL1*) is a transmembrane protein (14). *DLL1* plays a role in mediating cell fate decisions during hematopoiesis, and may participate in cell-to-cell communication (15). The uncontrolled activation of Notch1 signaling has been associated with developmental disorders and cancer (16,17), suggesting that Notch and its ligand may also be promising therapeutic targets (18). A previous study demonstrated that the increased expression of HPV E6 can trigger a decrease in Notch1 receptor activation in basal cells (19). However, the contribution of Notch1 and its δ-like ligands to the progression of cervical cancer, as well as the possible regulatory targets of this gene remain unclear.

Recently, the authors reported that seven miRNAs were highly expressed in cervical intraepithelial neoplasia grade 3 (CIN3), and two miRNAs had a low expression level in these samples (20). Among the highly expressed miRNAs, miR-130a-3p conferred a high risk for CIN3 lesions in liquid-based cytology cervical samples (20). In addition, other studies have demonstrated that miR-130a-3p plays a critical role in cervical cancer progression (21,22). Considering these findings, the aim of the present study was to evaluate the role of miR-130a-3p in cervical cancer progression *in vitro*.

Materials and methods

Cells, cell culture and transfection. A total of five commercial human cervical cancer cell lines (HeLa, SiHa, CaSki, C-4I and C-33A; American Type Culture Collection), a primary Brazilian cervical cancer immortalized cell line (HCB-514), kindly provided by the research group of R.M.R. [Rosa *et al* (23)] and a commercial non-tumorigenic epithelial cell line (HaCaT), kindly provided by the research group of Dr Laura Sichero and Dr Luisa Lina Villa (Center for Translational Investigation in Oncology, Instituto do Cancer do Estado de Sao Paulo, Hospital das Clinicas da Faculdade de Medicina da Universidade de São Paulo, São Paulo, Brazil) were used in the present study. All commercial cells were cultured in DMEM (Thermo Fisher Scientific, Inc.) supplemented with 10% fetal bovine serum (FBS) (Thermo Fisher Scientific, Inc.) in a humidified incubator with 5% CO_2 at 37˚C, while the primary cell line, HCB-514, was cultured as previously described (24). The cell lines were negative for mycoplasma contamination (MycoAlert Mycoplasma Detection Kit, Lonza Group, Ltd.; tested monthly) and were authenticated using short tandem-repeat analysis at the Molecular Oncology Research Center, Barretos Cancer Hospital facilities (Barretos, São Paulo, Brazil), as previously reported (24) (Table SI).

For functional analysis, the cells were seeded in six-well plates and cultured until reaching 70% confluency. Transfection was then performed using 20 nM anti-miR-130a-3p locked nucleic acid (LNA) inhibitor and a negative control A LNA (Qiagen, Inc.) in combination with 2.5 μl siPORT™ NeoFX™ transfection reagent (Thermo Fisher Scientific, Inc.), according to the manufacturer's protocol. According to the manufacturer, miRCURY LNA miRNA inhibitors are antisense oligonucleotides with perfect sequence complementary to their target. When introduced into cells, they sequester their miRNA target in highly stable heteroduplexes, effectively preventing the miRNA from hybridizing with its normal cellular interaction partners (25). Briefly, the adherent cells were trypsinized and resuspended in DMEM (Thermo Fisher Scientific, Inc.) containing 10% FBS and 1% streptomycin (Sigma-Aldrich; Merck KGaA) and penicillin (Sigma-Aldrich; Merck KGaA) and incubated at 37˚C for ≤1 h. The transfection reagent was diluted in Opti-MEM (Thermo Fisher Scientific, Inc.), as indicated in Table SII. Subsequently, the miR-130a-3p inhibitor (anti-miR-130a-3p, catalog number: 339122) and negative control A (identical to the former Scramble-miR control): No hits of >70% homology to any sequence in any organism in the NCBI and miRBase databases (cat. no. 339127) were diluted at a concentration of 20 μM in Opti-MEM (Thermo Fisher Scientific, Inc.), following the manufacturer's instructions. The diluted transfection agent and anti-miR-130a-3p were combined to form a transfection complex. Finally, the transfection complex and the cervical cancer cells were distributed in the plate according to the volumes indicated in Table SIII. Transfection was confirmed using reverse transcription-quantitative PCR (RT-qPCR). All subsequent experiments were performed after 48 h of transfection.

RNA isolation. Total RNA was extracted from the cervical cancer cells using the RecoverAll Total Nucleic Acid Isolation kit (cat. no. AM1975; Thermo Fisher Scientific, Inc) following the manufacturer's instructions. The purity and concentration of the total RNA were evaluated using a NanoDrop Spectrophotometer v3.7 (NanoDrop Technologies; Thermo Fisher Scientific, Inc.).

RT-qPCR. RT-qPCR was performed to detect the relative transcript levels of miR-130a-3p. Briefly, 10 ng total RNA were reverse transcribed into cDNA using MystiCq® microRNA cDNA Synthesis Mix (Sigma-Aldrich; Merck KGaA). qPCR was performed using SYBR®-Green I GoTaq® qPCR Master Mix (Promega Corporation) according to the manufacturer's instructions using the StepOnePlus™ Real-Time PCR System (Thermo Fisher Scientific, Inc.). In the reaction, 0.5 μl primers at 10 mg/ml were used (Table SIV). The cycling conditions of RT and qPCR are presented in the Table SV. The relative expression levels of miR-130a-3p were quantified based on the $2^{-\Delta\Delta Cq}$ method (26,27) and normalized to U6 (28).

Colony formation assay. Adhesion-independent cell proliferation was evaluated using colony formation assay. The transfected cervical cancer cells (CaSki and C-4I) were seeded in six-well plates at a density of 1,000 cells in 2 ml and were incubated for 14 days in a humidified incubator with 5% CO_2 at 37˚C. The medium was replaced every 7 days. Cell colonies were fixed with methanol (100%) and stained with crystal violet (Sigma-Aldrich; Merck KGaA) (0.1% in PBS) both for 10 min at room temperature. Colonies containing >50 cells were photographed under a light microscope (Eclipse 2200; (Nikon Corporation), and the number of colonies was analyzed using open-source software (OpenCFU; http://opencfu.sourceforge.net/) (29). The results are presented as the mean of ≥3

independent experiments and their respective standard deviations.

Transwell migration and invasion assays. The cell migratory and invasive abilities were evaluated using Transwell assay with a 24-well Transwell insert with an 8-μm pore size membrane (Corning, Inc.). For the invasion assay, the chambers were pre-coated with Matrigel solution (BD Biosciences). For the preparation of the inserts, Matrigel (BD Biosciences) was diluted at 1:10 in 0.01 M Tris buffer (pH 8.0) with 0.7% NaCl at 4˚C on ice. Subsequently, 100 μl diluted Matrigel were pipetted onto the membranes of each insert and incubated for 1 h in an oven at 37˚C. The excess fluid was removed, and the invasion assay was then carried out. For migration assay, Transwell assay was used with a 24-well Transwell insert with an 8-μm pore size membrane (Corning, Inc.) without Matrigel solution. The transfected cells ($2.5x10^4$ CaSki cells, and $4x10^5$ C-4I and HCB-514 cells) were seeded into the upper chamber in serum-free medium, while in the lower chamber, a serum-supplemented medium (DMEM culture medium + 10% FBS) (Thermo Fisher Scientific, Inc.) was added for both assays. Following incubation for 24 h in a humidified incubator with 5% CO_2 at 37˚C, those cells that had migrated or invaded the lower surface of the membrane were fixed with methanol (100%), stained with crystal violet (0.1%) both for 10 min at room temperature.. The Transwell inserts were photographed under a light microscope (Eclipse 2200; Nikon Corporation), and the number of cells was analyzed with the open-source software CFU (http://opencfu.sourceforge.net/). The results are represented as the mean of ≥3 independent experiments.

Wound healing assay. The alteration of cell migration induced by miR-130a-3p inhibition was also evaluated using a wound healing assay. The transfected CaSki and C-4I cells were seeded in six-well plates at a density of $1x10^6$ cells/ml. When the cells were confluent, a scratch was made on the monolayer using a sterile plastic 1,000-μl pipette tip. The cells were washed three times with PBS, and complete medium with 0.5% FBS was then added. Supplementation with FSB was maintained due to transfection with the inhibitors or the negative control. Other studies have also used FSB supplementation in the wound healing assay (30,31). Images of the scratch were captured at x10 magnification at 0, 24, 48 and 72 h using an Olympus IX71 inverted microscope (BioTek Instruments, Inc.). The widths of the scratches were measured using ImageJ Software version 1.49 (National Institutes of Health). The relative migration distance was calculated as previously described (32).

Gene expression profiling. To verify the differentially expressed genes in cervical cancer cells, the HCB-514 cell line was selected and compared with the non-tumorigenic epithelial cell line HaCat. For gene expression profiling, the nCounter® Analysis System (NanoString Technologies, Inc.) was used with nCounter® PanCancer Pathways panel, which comprises 730 cancer pathway-related genes in addition to 40 housekeeping genes curated from data in The Cancer Genome Atlas (TCGA), as well as six positive and eight negative controls. All procedures regarding sample preparation, hybridization, detection and scanning were performed according to the manufacturer's instructions (NanoString Technologies, Inc.) (33). Briefly, 100 ng RNA from HCB-514 or HaCaT cells was incubated with reporter and capture probes for 21 h at 65˚C. Subsequently, the hybridized samples were automatically purified and loaded into a cartridge in nCounter® PrepStation (NanoString Technologies, Inc.). Finally, the cartridge containing immobilized and aligned reporter complexes was transferred to nCounter® Digital Analyzer (NanoString Technologies, Inc.), with 280 fields of view. Raw data were collected and pre-processed using nSolver™ Analysis Software v4.0 (NanoString Technologies, Inc.), and further normalization and differential expression analysis were performed using R-project v3.6.3 (The R Foundation). Data were normalized using the housekeeping method with the NanoStringNorm package (Bioconductor) (https://www.bioconductor.org/). Normalized data were log2-transformed and used as input for differential expression analysis. *DLL1* and *WNTA10A* expression validation upon transfection of the HCB-514 cells with anti-miR-130a-3p and the negative control was evaluated from counts of the expression of these genes using the nCounter® PanCancer Pathways panel. Data were normalized with the housekeeping method using the *GPATCH3* and *TRIM39* genes. The gene expression data are available on the National Center for Biotechnology Information (NCBI)-Gene Expression Omnibus (GEO) platform (https://www.ncbi.nlm.nih.gov/geo/query/acc.cgi) under the Accession no. GSE224301.

In silico target prediction and pathways enrichment. The bidirectional analysis between miR-130a-3p and differentially expressed genes was performed using the online tool MicroRNA Data Integration Portal (mirDIP) v.5.1.16.1 (34) to predict a suitable target for miR-130a-3p. The top 5% of target genes were considered as the high score. By searching for potential miRNAs, the miR-130a-3p targeting site was identified within the 3' untranslated region (UTR) of DLL1 and Wnt Family Member 10A (*WNT10A*), as detected using TargetScan version 8.0 (http://www.targetscan.org) (35). Subsequently, to determine the association between miRNA targets and cervical cancer, the plugin ReactomeFI on Cytoscape version 3.9.1 (https://cytoscape.org/) was employed. Molecular pathways enrichment was performed with a false discovery rate (FDR)-corrected P-value of $P<0.001$. The interaction network was performed using Cytoscape (36).

External in silico validation of DLL1 and WNT10A genes. To evaluate the expression status of DLL1 and *WNT10A* genes in cervical squamous cell carcinoma and endocervical adenocarcinoma (CESC) samples compared with 13 normal cervical tissues, TCGA and The Genotype-Tissue Expression datasets available in the Gene Expression Profiling Interactive Analysis (GEPIA) 2 database (http://gepia2.cancer-pku.cn/#index) were used (37). These databases provided 13 normal samples for comparison with 306 CESC tissue samples. For the validation of DLL1 and *WNT10A* gene expression in a panel of cervical cancer cell lines (HeLa, SiHa, CaSki, C-4I and C-33A) compared with the HaCaT cell line, gene expression data available on the Gene Expression patterns across Normal and Tumor tissues (GENT) 2 platform (http://gent2.appex.kr/gent2/) were used (38).

Gene set enrichment analysis (GSEA). All expressed genes, regardless of whether they were differentially expressed in either case, were used for GSEA analysis. Gene set analysis was analyzed using GSEA software (http://software.broadinstitute.org/gsea/index.jsp) (39,40) based on KEGG gene set collections (MSigDB v7.0, Broad Institute) (41,42). GSEA first ranked all expressed genes according to the significance of differential gene expression between the HCB-514 and HaCaT cells. The enrichment score (ES) for each gene set is then calculated using the entire ranked list, which reflects how the genes for each set are distributed in the ranked list. Normalized enriched score (NES) was determined for each gene set (39). The significant enrichment of gene set was selected based on the absolute values of NES >1, nominal P-value of NES ≤0.05 and rate FDR ≤0.05.

Statistical analysis. Single comparisons between the conditions studied were performed using an unpaired Student's t-test, while comparisons between multiple groups were performed using ANOVA and Tukey's post hoc. For the analysis of differential gene expression, the Student's t-test was used, and P<0.01 corrected by FDR and FC≥2 was considered. For the correlation analysis, the Spearman's correlation was used. Significantly enriched pathways terms are shown in -log10 with Benjamini-Hochberg false discovery rate-corrected P-values. Statistical analyses were performed using GraphPad Prism version 9.0.0 (GraphPad Software; Dotmatics). P<0.05 was considered to indicate a statistically significant difference. The results are represented as the mean of ≥3 independent experiments.

Results

miR-130a-3p is highly expressed in cervical cancer cell lines. The relative expression levels of miR-130a-3p in cervical cancer cell lines and a non-tumorigenic epithelial cell line were determined using RT-qPCR. Following log-scale normalization, miR-130a-3p expression was found to be significantly higher in the cervical cancer cell lines, HeLa (P=0.0332), SiHa (P=0.0021), CaSki (P=0.0001), C-4I (P=0.0002) and HCB-514 (P=0.0002), compared with that in the non-tumorigenic epithelial cell line, HaCaT (Fig. 1). The CaSki, C-4I and HCB-514 cell lines were further selected for subsequent functional analyses.

Anti-miR-130a-3p knocks down the expression of miR-130a-3p in cervical cancer cells. The expression of miR-130a-3p was detected using RT-qPCR following transfection with anti-miR in the CaSki, C-4I and HCB-514 cells. As shown in Fig. 2, in the cervical cancer cell lines, miR-130a-3p expression was lower in the anti-miR-130a-3p group than in the negative control cells (P<0.0001).

Anti-miR-130a-3p inhibits the proliferation of cervical cancer cells. The proliferative ability of the CaSki and C-4I cells was evaluated using colony formation assay. The results demonstrated that the ability of a single cell to form colonies was reduced following the inhibition of miR-130a-3p in the CaSki (81%; P=0.0100) and C-4I (69.5%; P<0.0001) cells compared with that in the negative control group (Fig. 3).

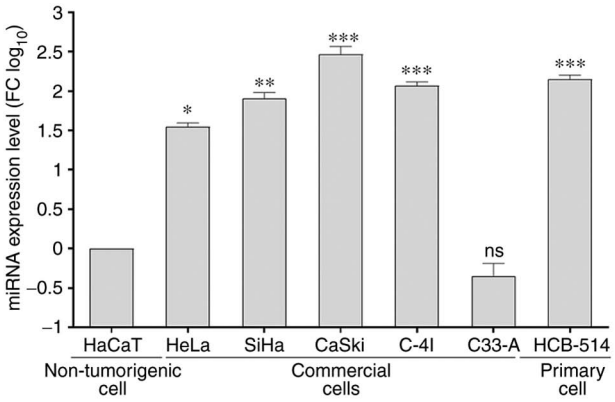

Figure 1. miR-130a-3p is highly expressed in cervical cancer cells. The HeLa, SiHa, CaSki, C-4I and HCB-514 cell lines had a significantly higher expression of miR-130a-3p than the non-tumorigenic epithelial cell line, HaCaT. Bars represent the standard deviation. *P<0.05, **P<0.01 and ***P<0.001, vs. HaCaT cells. ns, not significant; miR, microRNA.

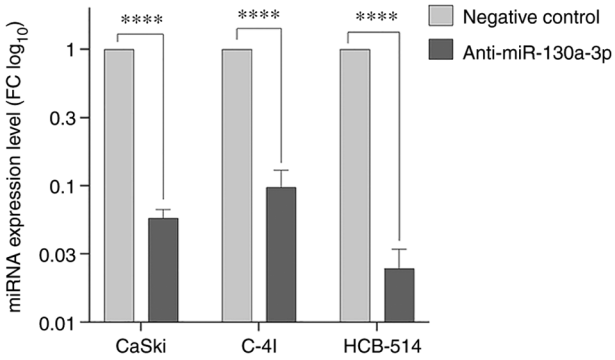

Figure 2. Anti-miR-130a-3p knocks down the expression of miR-130a-3p in cervical cancer cells. The expression of miR-130a-3p in CaSki, C-4I and HCB-514 cells following transfection was reduced, indicating that anti-miR-130a-3p suppressed the expression of miR-130a-3p. The bars represent the standard deviation. ****P<0.0001. miR, microRNA.

Anti-miR-130a-3p inhibits cervical cancer cell migration. To evaluate the ability of cervical cancer cells to migrate, Transwell assays were performed in the absence of Matrigel. Anti-miR-130a-3p inhibited the migration of the CaSki, C-4I and HCB-514 cells by 55% (P=0.0012), 11.3% (P<0.0001) and 33.3% (P<0.0001), respectively, compared with that of negative control cells (Fig. 4).

In the wound healing assay, the open wound in the control group was narrowed at 48 h in the CasKi cells (Fig. S1A) and at 24 h in the C-4I cells (Fig. S1B). However, after knocking down miR-130a-3p in these cell lines, the scar healing rate was markedly attenuated. It was possible to observe the almost complete healing of the wound at 72 h in the negative control group, while in the anti-miR-130a-3p group, the wound was not completely healed. Moreover, the distance between the wound edges decreased at a slower rate in the anti-miR-130a-3p group than in the negative control group. These results indicated that anti-miR-130a-3p suppressed the migration of cervical cancer cells.

Anti-miR-130a-3p inhibits cervical cancer cell invasion. The present study also examined the *in vitro* invasiveness of CaSki, C-4I and HCB-514 cells transfected with anti-miR-130a-3p or

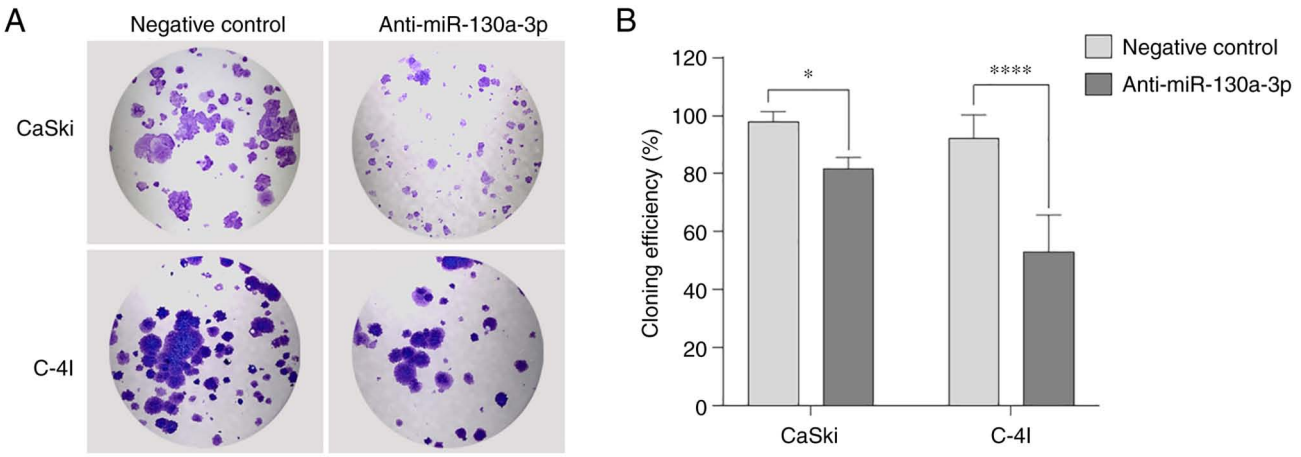

Figure 3. Anti-miR-130a-3p inhibited the proliferation of cervical cancer cells. Colony formation assay was used to evaluate the proliferation of CaSki and C-4I cells, which exhibited a reduced clone number in the anti-miR-130a-3p group. (A) Images of the colony formation assay. (B) Bar plots of the data from panel A. Bars represent the standard deviation. *P<0.05 and ****P<0.0001. miR, microRNA.

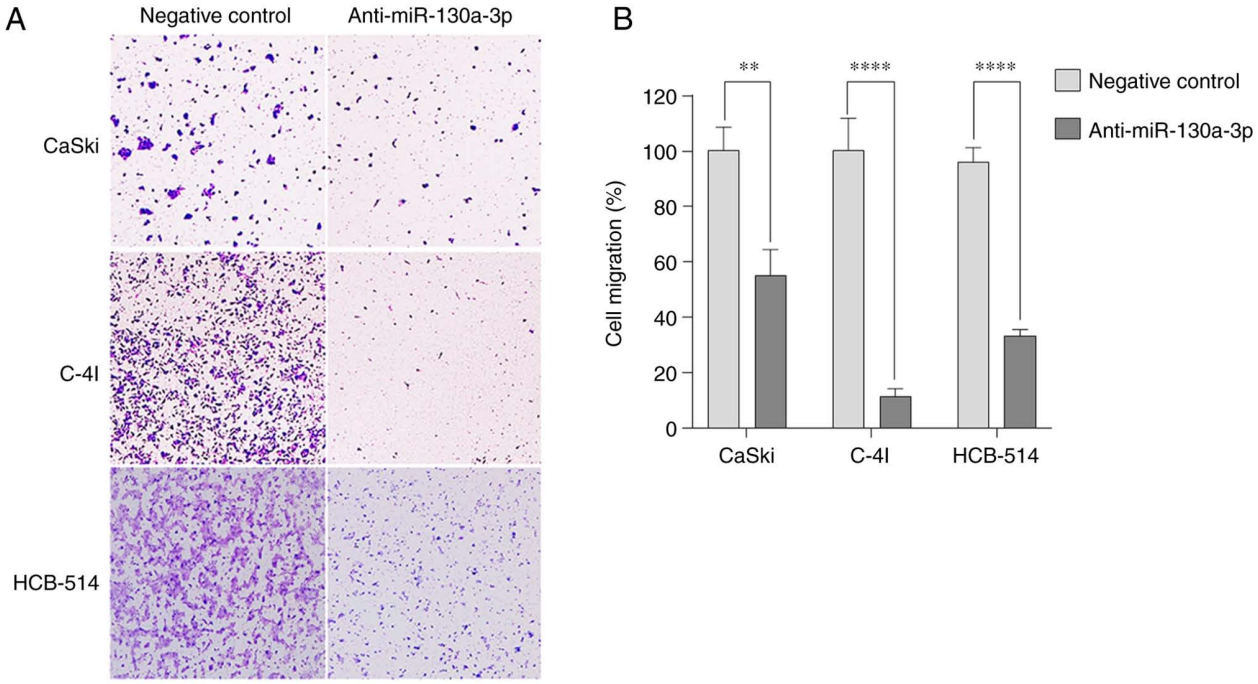

Figure 4. Anti-miR-130a-3p inhibits the migration of cervical cancer cells. (A) Images of Transwell assay in CaSki, C-4I and HCB-514 cell lines, which exhibited a decreased migration after miR-130a-3p was knocked down. (B) Bar plots of the data from panel A. Bars represent the standard deviation. **P<0.01 and ****P<0.0001. miR, microRNA.

negative control using Matrigel invasion assay. Cell invasion was measured by the number of cells that migrated through the Matrigel insert. Anti-miR-130a-3p inhibited the invasion of the CaSki, C-4I and HCB-514 cells by 30.7% (P<0.0001), 26.3% (P<0.0001) and 30.7% (P<0.0001), respectively, compared with that of the negative control cells (Fig. 5). These data suggested that miR-130a-3p contributed to the invasiveness of cervical cancer cells.

Gene expression profile in HCB-514 cells. Gene expression analysis using nCounter® PanCancer Pathways revealed a different gene expression profile between HCB-514 cells and the HaCaT control cell line (FC≥2 and P<0.01; Fig. 6). The differential genes expressed were then filtered using a P-value corrected by FDR <0.01. In total, 22 differentially expressed genes were identified. Among these 22 genes, 15 genes (*CCND2, FST, INHBA, BMP7, BMP4, CACNG4, SOX9, TNC, DUSP6, WNT10A, DLL1, ITGB7, CARD11, CCND1* and *CDK6*) were significantly downregulated in the HCB-514 cells compared with the HaCaT cell line, while seven genes (*IL12RB2*, *IL6R*, *ANGPT1*, *PTPRR*, *TLR2*, *PAX8* and *COL4A3*) were upregulated (Table I).

In silico analysis demonstrates that DLL1 and WNT10A are a decoy of miR-130a-3p to CESC progression. mirDIP v.5.1.16.1 predicted that, among the 22 differentially

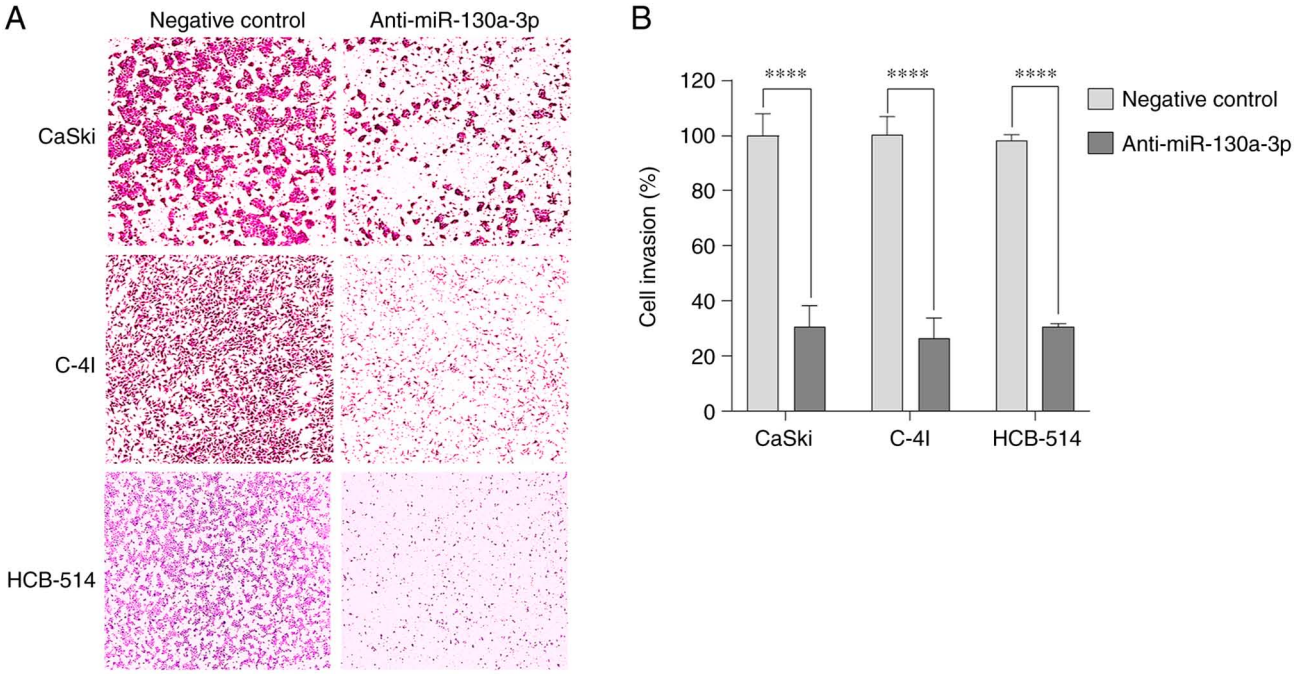

Figure 5. Anti-miR-130a-3p inhibits the invasion of cervical cancer cells. (A) Images of Transwell assay in the CaSki, C-4I and HCB-514 cell lines, which exhibited a decreased invasion after miR-130a-3p was knocked down. (B) Bar plots of the data from panel A. Bars represent the standard deviation. ****P<0.0001. miR, microRNA.

expressed genes identified usin nCounter® technology (Table I), *DLL1* and *WNT10A* could be targeted by miR-130a-3p (Table II). To establish whether the *DLL1* and *WNT10a* genes could affect cervical cancer progression, TargetScan 7.1 was initially used to confirm an interaction site of *DLL1* or *WNT10A* with miR-130a-3p. As illustrated in Fig. 7A, a potential binding site for miR-130a-3p was found in the 3'UTR regions of both mRNAs. The GEPIA2 database was then used to examine the expression of *DLL1* and *WNT10A* genes. It was found that the *DLL1* gene was notably expressed at low levels in CESC tissues compared with normal tissues (Fig. 7B). However, the *WNT10A* gene was upregulated in CESC tissues compared with normal tissues (Fig. 7C). In addition, using the GEPIA 2 database, the expression of the *DLL1* and *WNT10A* genes in patients with different stages of CESC was evaluated, although no statistically significant differences between the groups were observed; however, a trend towards a decrease in expression was observed for the *DLL1* and *WNT10A* genes in the advanced stages of CESC (Fig. 7D and E).

The present study also evaluated the *DLL1* and *WNT10A* expression levels in cervical cancer cell lines using data on gene expression available in the GENT2 platform (http://gent2.appex.kr/gent2/). Significantly low levels of *DLL1* expression were observed in the CaSki, SiHa, C-4I and HeLa cells in comparison with those in the HaCaT cells (Fig. 7F). Similar results were found for the *WNT10A* gene, since all the cervical cell lines exhibited a decrease in *WNT10A* expression compared with the HaCaT cells (Fig. 7G). Although Spearman's correlation analyses did not reveal any significant differences, there was a tendency for a negative correlation between the levels of miR-130a-3p and the *DLL1* gene (Spearman's Rho=-0.4086, P=0.0659; Fig. 7H), and the *WNT10A* gene (Spearman's Rho=-0.2589, P= 0.0.2572; Fig. 7I) in a cervical cancer cell line panel.

Subsequently, enrichment analysis was performed using Cytoscape software with the Reactome plugin of the *DLL1* and *WNT10A* genes to gain insights into the pathways that are affected in CESC progression (Fig. 7J and Table SVI). It was found that the downregulated *DLL1* gene in CESC and cervical cancer cell lines was significantly enriched in the pathway of proteolysis and signaling pathway of Notch, pathways in cancer, signaling by Notch2 and 3, presenilin action in Notch and Wnt signaling, Notch signaling pathway, signaling by NOTCH1, T helper (Th)1 and Th2 cell differentiation, and endocrine resistance. The *WNT10A* gene was significantly enriched in pathways in cancer, Wnt ligand biogenesis and trafficking, basal cell carcinoma, cadherin signaling pathway, signaling pathways regulating pluripotency of stem cells, mTOR signaling pathway, Hippo signaling pathway, Wnt signaling pathway, hepatocellular carcinoma, proteoglycans in cancer, and Wnt signaling pathway (Fig. 7J and Table SVI).

To validate whether *DLL1* and *WNT10A* expression was also altered due to miR-130a-3p inhibition, the expression of DLL1 and WNT10A was evaluated in the HCB-514 cells following miR-130a-3p inhibition. It was observed that both for the *DLL1* gene (FC=3.03, P=0.0089) and for the *WNT10A* gene (FC=4.22, P<0.001), there was a significant increase in expression when the cells were subjected to the inhibition of miR-130a-3p in comparison to their respective negative controls (Fig. S2).

GSEA. The difference in gene expression levels between the HCB-514 and HaCaT cells was further investigated using GSEA. GSEA was performed using a KEGG-based list, including 186 gene sets. In total, 64 KEGG-based gene sets, were identified as significantly enriched (FDR <0.05;

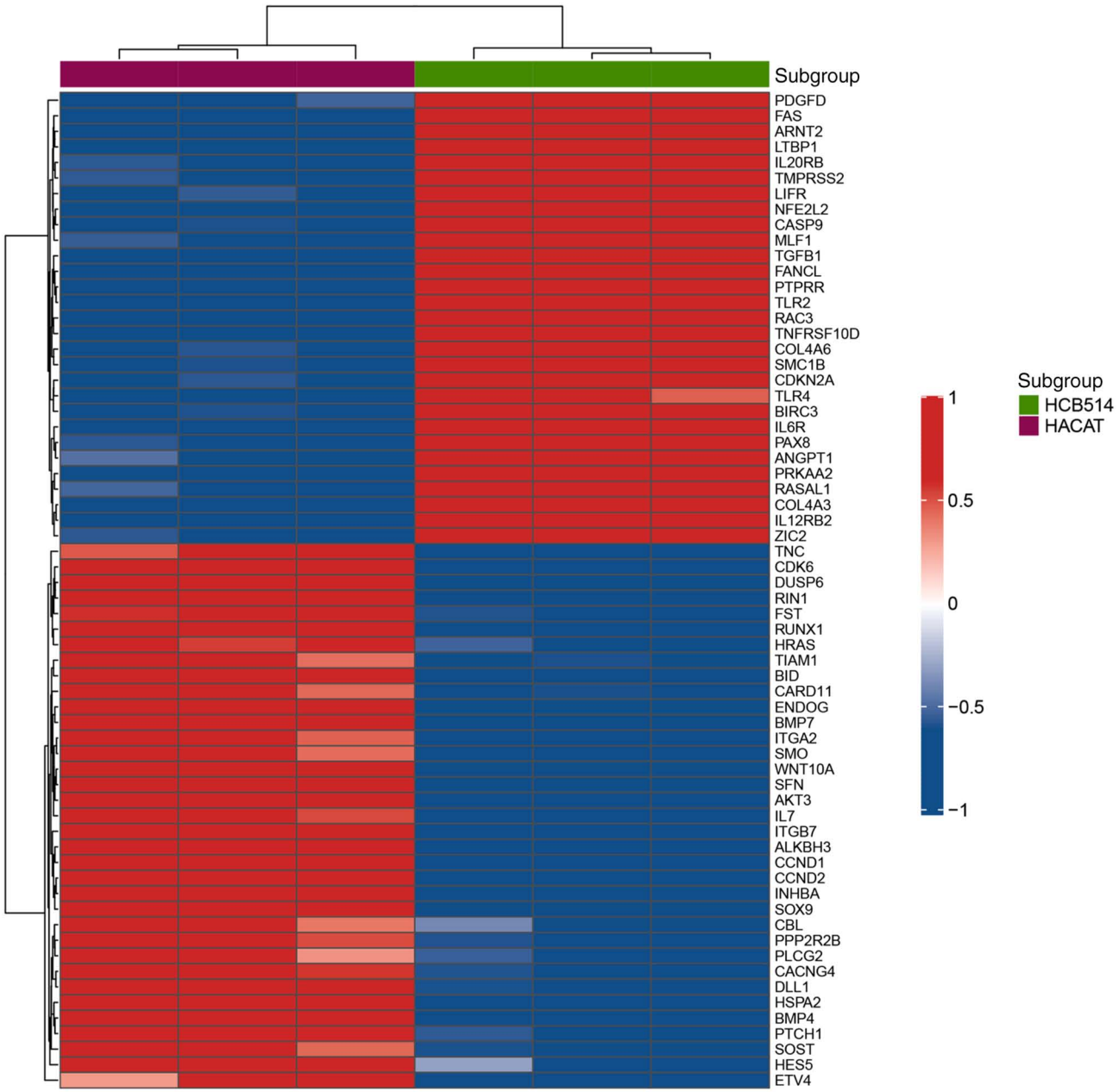

Figure 6. Gene expression profile in HCB-514 cells using nCounter® technologies. Heatmap was used for gene expression profiling of the HCB-514 primary cell line vs. HaCaT control cells. Cell lines were arranged in columns, while gene expression levels were arranged in rows, and both were hierarchically clustered using the Euclidean distance with the average linkage of nodes. Red shades indicate an increased relative expression, while blue shades indicate a reduced expression. The bars above indicate the groups used for the analysis. Purple indicates samples from the HaCaT control cells (n=3), while green refers to the HCB-514 cells (n=3) (FC≥2; P<0.01).

Table III). NES indicates expression values in HCB-514 vs. HaCaT cells. Of note, from the KEGG-based list, all gene sets which demonstrated a high expression in the HCB-514 cells were mainly related to 'gap junction' (Fig. 8A), 'calcium signaling pathway' (Fig. 8B), 'long-term potentiation' (Fig. 8C) and 'apoptosis' (Fig. 8D).

Discussion

The aberrant expression of miR-130a-3p in different tumor types suggests that this miRNA may play distinct roles in tumorigenesis, depending on the cell type involved. The role of miR-130a-3p in tumor development and progression appears to be contradictory, as it may serve as an oncogene or a tumor suppressor gene, regulating various canonical signaling pathways or target genes (43). Previous research has demonstrated that miR-130a-3p is upregulated in CIN3 (20). In addition, studies performing the assessment of miR-130a-3p expression in cervical cancer tissue samples identified an overexpression of this miRNA in comparison with that in normal samples (22,43,44). The findings of the present study demonstrated that miR-130a-3p was highly expressed in HPV-positive cervical cancer cell lines and played a regulatory role. Thus, the present study evaluated the effects of miR-130a-3p inhibition on CaSki, C-4I and HCB-514 cells. These cell lines were selected as they exhibited a significantly

Table I. Genes differentially expressed in HCB-514 cells compared to the HaCaT control cell line using a NanoString Technologies analysis system.

Gene	Fold change	Status	P-value	FDR P-value
CCND2	-8.0	Downregulated	0.0001	0.0089
FST	-6.5	Downregulated	0.0019	0.0350
INHBA	-5.7	Downregulated	0.0020	0.0350
BMP7	-5.3	Downregulated	0.0004	0.0200
BMP4	-5.0	Downregulated	0.0023	0.0350
CACNG4	-4.4	Downregulated	0.0022	0.0350
SOX9	-4.4	Downregulated	<0.0001	0.0041
TNC	-4.2	Downregulated	0.0038	0.0490
DUSP6	-4.0	Downregulated	0.0016	0.0330
WNT10A	-4.0	Downregulated	0.0022	0.0350
DLL1	-3.2	Downregulated	0.0012	0.0330
ITGB7	-2.2	Downregulated	0.0006	0.0200
CARD11	-2.1	Downregulated	0.0036	0.0480
CCND1	-2.0	Downregulated	<0.0001	0.0041
CDK6	-2.0	Downregulated	0.0002	0.0130
IL12RB2	2.2	Upregulated	0.0006	0.0200
IL6R	2.3	Upregulated	0.0006	0.0220
ANGPT1	3.2	Upregulated	0.0036	0.0480
PTPRR	4.1	Upregulated	<0.0001	0.0041
TLR2	4.3	Upregulated	0.0002	0.0120
PAX8	4.8	Upregulated	0.0014	0.0330
COL4A3	5.2	Upregulated	0.0013	0.0330

The Student's t-test was used for statistical analysis. FDR P-value, P-value corrected by false discovered rate.

higher expression of miR-130a-3p at the basal level than others. Furthermore, the C-33A cell line exhibited a low level of miR-130a-3p expression. Although previous studies reporting the low expression of miR-130a-3p in C-33A cells are limited, it may be hypothesized that the high expression of miR-130a-3p may be associated with the presence of HPV, since C-33A is a negative-HPV cell line. Therefore, further studies are warranted to confirm this hypothesis.

The transient transfection of anti-miR-130a-3p suppressed adhesion-independent cell proliferation, migration and invasion in cervical cancer cells by decreasing the expression of miR-130a-3p. In agreement with the findings of a previous study, decreasing the expression of miR-130a-3p also inhibited cell proliferation. Furthermore, that study demonstrated that the inhibition of miR-130a-3p was responsible for the radiosensitivity of non-small cell lung cancer (45), while another study demonstrated that miR-130a-3p aggravated gastric cancer cell proliferation, migration and invasion by reducing *GCNT4* expression and activating the TGF-β1/SMAD3 signaling pathway (46).

The findings of the present study support the results identified in other studies on the contribution of miR-130a-3p to cervical tumor progression. Fan *et al* (23) observed that miR-130a 3p expression levels were higher in cervical tumor tissues compared with those in healthy tissues. Moreover, that study verified that miR-130a-3p knockdown inhibited cervical cell proliferation and invasion *in vitro* and *in vivo* compared with the negative control group.

Other studies have demonstrated that miR-130-3p expression levels can affect the therapeutic response. Huang *et al* (47) performed a study on 50 patients with breast cancer before and after epirubicin-based neoadjuvant chemotherapy. They revealed that the increased expression of miR-130a enhanced the sensitivity of breast cancer cells to doxorubicin, and that the inhibition of miR-130a expression may be associated with resistance to epirubicin-based chemotherapy in breast cancer tissues. It has been reported that miR-130a-3p regulates *SMAD4* expression in hepatocellular carcinoma cells, and this regulatory axis plays a critical role in gemcitabine-mediated sensitivity, in which the overexpression of miR-130a-3p leads to an increase in the sensitivity to gemcitabine of these cells (48). Therefore, the expression of miR-130a-3p is also associated with the treatment administered.

Furthermore, the present study investigated the role that miR-130a-3p plays in cervical cancer progression. The results of colony formation assay revealed that miR-130a-3p inhibition significantly reduced the proliferation of CaSki and C-4I cells. Wound healing and Transwell assays were performed to investigate the mechanisms through which anti-miR-130a-3p affects the migration of cervical cancer cells, and it was found that anti-miR-130a-3p inhibited cell migration. The results from the Transwell invasion assay demonstrated that anti-miR-130a-3p reduced the invasion of cervical cancer cells. The aforementioned findings are in accordance with those of previous studies reporting that miR-130a-3p may function as a tumor promoter (22,45,46).

Bioinformatics analysis predicted that *DLL1* and *WNT10A* may be one of the targets of miR-130a-3p. This observation was supported by *in silico* analyses that demonstrated the reduced expression of *DLL1* in patients with CESC and in a panel of cervical cancer cell lines. However, there was no reduction in expression in patients with CESC, although analyses using online databases revealed a significant reduction in *WNT10A* expression in cervical cancer cells. Previous findings have demonstrated that both Notch1 mutation and inhibition induced by HPV E6 in cervical cancer can drive neoplastic development in stratified squamous epithelia. However, the contribution of Notch1 and its d-like ligands to the susceptibility and progression of cervical cancer remains poorly understood (19). In comparison with the results of the present study, Liu *et al* (48) identified that miR-130b inhibited the upstream gene, leading to a decrease in the expression of Notch-DLL1, which enhanced the invasion and metastasis of liver cancer cells. Taken together, these results suggest that *DLL1* may be the target gene for miR-130a-3p, which is involved in the proliferation, migration and invasion of cervical cancer cells *in vitro*.

By contrast, herein, *in silico* analysis revealed that, although *WNT10A* could be a target of miR-130a-3p, the *WNT10A* gene exhibited increased expression in patients with CESC, and was expressed at low levels in cervical cancer cells, in which cervical cancer cells demonstrated the overexpression of miR-130a-3p. In addition, the present study validated the differential expression of *DLL1* and *WNT10A* between the

A

	Predicted consequential pairing of target region (top) and miRNA (bottom)	Site type	Context++ score	Context++ score percentile	Weighted context++ score	Conserved branch length	PCT
Position 73-79 of DLL1 3'UTR	5' . . . UCCGUGACGUCGCCGUUGCACUA . . .	8 mer	-0.28	95	-0.28	4.810	0.90
hsa-miR-130a-3p	3' UACGGGAAAAUUGUAACGUGAC						
Position 495-501 of WNT10A 3'UTR	5' . . . UAACAAAUAUUUAUU- -UUGCACUC. . .	8 mer-m8	-0.34	98	-0.34	3.917	0.68
hsa-miR-130a-3p	3' UACGGGAAAGUAGUAACGUGAC						

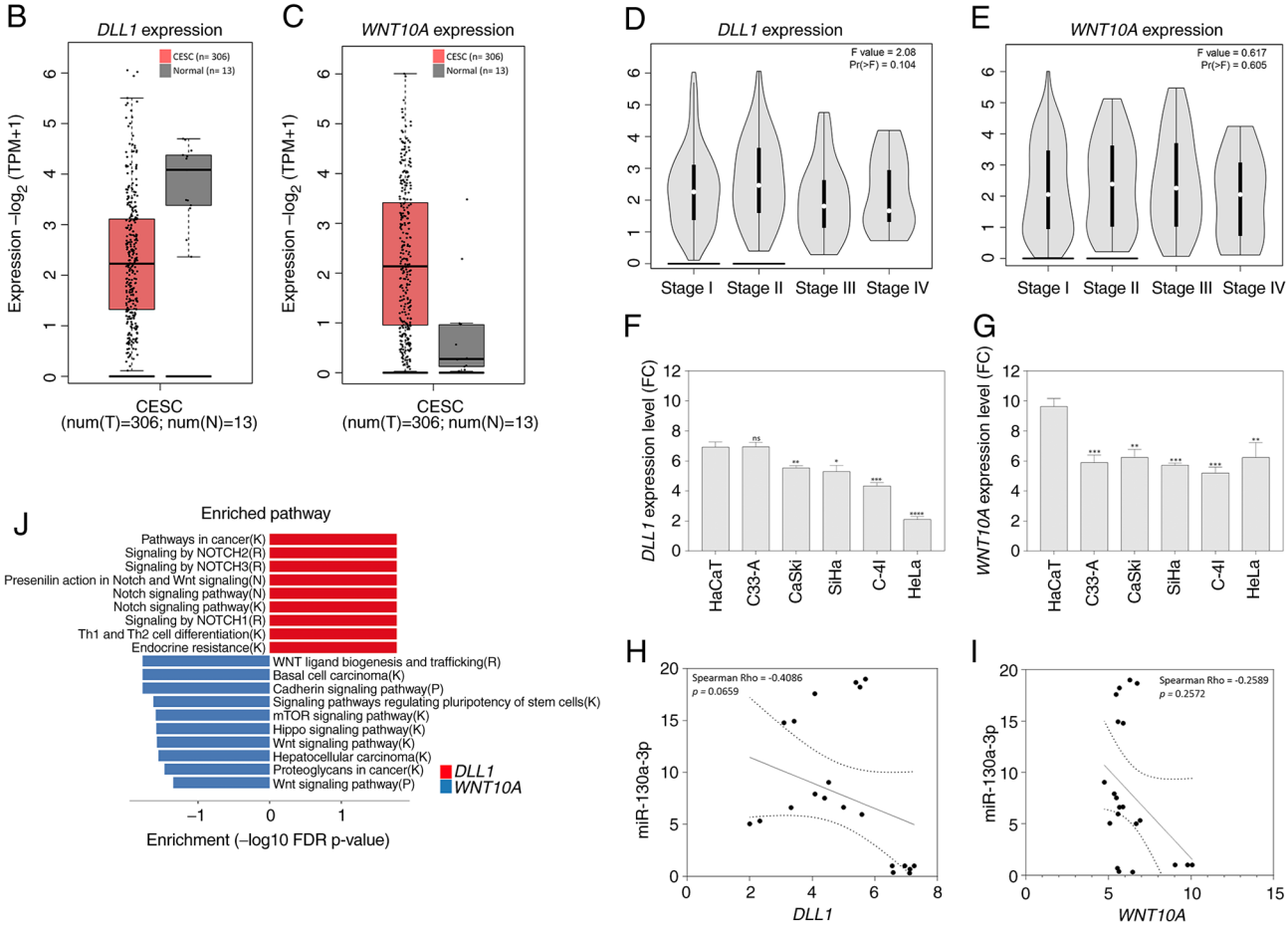

Figure 7. *In silico* analysis of *DLL1* and *WNT10A*, and their association with the progression of patients with CESC and with cervical cancer cell lines. (A) Putative miR-130a-3p binding site in the 3'untranslated regions of *DLL1* and *WNT10A*, as predicted using TargetScan. (B,C) Expression boxplots of the genes using the GEPIA2 database (P<0.05; CESC tissues, n=306; normal tissues, n=13) (B) *DLL1* expression; (C) *WNT10A* expression. (D) Association between *DLL1* expression, and pathological stage in patients with CESC using the GEPIA2 database (P<0.05). (E) Association between *WNT10A* expression, and pathological stage in patients with CESC using the GEPIA2 database (P<0.05). (F) Data from the GENT2 database regarding *DLL1* expression in a cervical cancer cell line panel in comparison with HaCaT cells. ns, not significant. *P<0.05, **P<0.01, ***P<0.001 and ****P<0.0001. (G) Data from the GENT2 database regarding *WNT10A* expression in a cervical cancer cell line panel in comparison with HaCaT cells. **P<0.01, ***P<0.001. (H,I) Spearman's pair-wise correlation analysis of miRNA-mRNA target pairs in cervical cancer cell lines paired in triplicate (n=5). (H) Correlation analysis revealed that increased miR-130a-p expression levels were associated with *DLL1* downregulation in cervical cancer cell lines. In the correlation plots, the solid line represents the least square estimate, and P-values represent global significance P<0.05; (I) correlation analysis revealed that increased miR-130a-p expression levels were associated with *WNT10A* downregulation in cervical cancer cell lines. In the correlation plots, the solid line represents the least square estimate, and P-values represent global significance P<0.05. (J) Enrichment pathways using the *DLL1* (right panel, red) and *WNT10A* (left panel, blue) genes in CESC. Significantly enriched pathways terms are shown in -log10 with Benjamini-Hochberg false discovery rate-corrected P-values. The letter in parentheses after each pathway gene set name corresponds to the source of the pathway annotations. B, BioCarta; K Kyoto Encyclopedia of Genes and Genomes; R, Reactome; P, Panther; CESC, cervical squamous cell carcinoma and endocervical adenocarcinoma; miR, microRNA; GEPIA, Gene Expression Profiling Interactive Analysis; *DLL1*, δ-like Notch1 ligand.

HCB-514 cells with miR-130a-3p inhibition in comparison with negative control A. This result revealed that the modulation of miR-130a-3p expression was capable of causing a change in the expression of both evaluated genes.

Thus, these results suggest that the *WNT10A* gene may not be the main target of miR-130a-3p. It has been demonstrated that miRNAs can regulate the expression of the *WNT10A* gene. Yu *et al* (49) reported that the *WNT10A* gene, a member of the Wnt/β-catenin signaling pathway, was confirmed to be a target of miR-378a-3p. It has been observed that the inhibition of miR-378a-3p expression contributes to the activation of hepatic stellate cells, which led to increased cell proliferation, and the expression of α-smooth muscle actin and collagen (49). Moreover, it has been demonstrated that miR-361-3p mediates tumor inhibition in lymphoma, and this regulation can be ascribed to the upregulation of *WNT10A* that was identified in lymphoma cell lines and normal lymphocytes (50).

Table II. Bidirectional target prediction for differentially expressed genes and miR-130a-3p using the mirDIP tool.

Gene	Uniprot	Rank	Source	Confidence score
DLL1	O00548	0.6302500	miranda_May_2021	0.0210342
DLL1	O00548	0.8863533	mirbase	0.0417327
DLL1	O00548	0.0976322	mirzag	0.0881644
DLL1	O00548	0.2058031	miRDB_v6	0.0930805
DLL1	O00548	0.8913646	miRTar2GO	0.1264211
DLL1	O00548	0.3556803	MBStar	0.0339947
DLL1	O00548	0.0055481	MirAncesTar	0.1070419
DLL1	O00548	0.7009731	MiRNATIP	0.0196684
DLL1	O00548	0.4255360	MultiMiTar	0.1111873
DLL1	O00548	0.7303563	RNA22	0.0136887
DLL1	O00548	0.2063430	TargetScan_v7_2	0.3306254
WNT10A	Q9GZT5	0.4518441	miranda_May_2021	0.0254858
WNT10A	Q9GZT5	0.6573457	mirbase	0.0465710
WNT10A	Q9GZT5	0.3362469	mirzag	0.0564491
WNT10A	Q9GZT5	0.9904704	miRDB_v6	0.0602461
WNT10A	Q9GZT5	0.4086939	miRTar2GO	0.1266619
WNT10A	Q9GZT5	0.0046046	MirAncesTar	0.1103192
WNT10A	Q9GZT5	0.4074708	MultiMiTar	0.1126795
WNT10A	Q9GZT5	0.1128482	TargetScan_v7_2	0.3892957

DLL1, delta-like Notch1 ligand; *WNT10A*, Wnt family member 10a.

Table III. Gene set enrichment analysis between the HCB-514 and HaCaT cells.

Gene set	NES	NOM P-value	FDR P-value	Genes
Gap junction	0.0481	<0.001	0.042	*PDGFD*, *PLCB1*, *PRKCA*, *PRKX*, *SOS1*, *NRAS*, *MAP2K1*, *SOS2*, *GNAS*, *MAPK3*, *PRKACB*, *RAF1*, *GRB2*, *PRKACA*, *EGFR*, *PDGFC*, *MAP2K2*, *GNA11*, *KRAS*, *MAPK1*, *GNAQ*, *HRAS*, and *PDGFA*
Calcium signaling pathway	0.0470	<0.001	0.036	*PLCB1*, *PRKCA*, *PRKX*, *PLCE1*, *PPP3CA*, *GNAS*, *PPP3R1*, *PRKACB*, *PPP3CC*, *PRKACA*, *EGFR*, *ERBB2*, *GNA11*, *PPP3CB*, *GNAQ*, and *PLCG2*
Long-term potentiation	0.0455	<0.001	0.033	*PLCB1*, *PRKCA*, *PRKX*, *NRAS*, *PPP3CA*, *MAP2K1*, *EP300*, *MAPK3*, *BRAF*, *PPP3R1*, *PRKACB*, *RAF1*, *PPP3CC*, *PRKACA*, *MAP2K2*, *KRAS*, *MAPK1*, *PPP3CB*, *GNAQ*, and *HRAS*
Apoptosis	0.0372	<0.001	0.054	*IRAK3*, *BIRC3*, *IRAK2*, *CASP9*, *IL1A*, *TNFRSF10*, *PRKX*, *FAZ*, *TNFSF10*, *TNFRSF10*, *PIK3CA*, *IL1R1*, *AKT2*, *NFKBIA*, *PIK3CD*, *PPP3CA*, *PIK3R1*, *BAX*, *NFKB1*, *CASP7*, *IL1B*, *CHUK*, *IL1RAP*, *PPP3R1*, *BCL2L1*, *PRKACB*, *PPP3CC*, *CAPN2*, *PIK3R3*, *PIK3CB*, *PRKACA*, *IKBKB*, *CASP3*, *AKT1*, *PRKAR2A*, *RELA*, *PPP3CB*, *IKBKG*, *TNFRSF10*, *BAD*, *TP53*, *CASP8*, *PIK3R2*, *MAP3K14*, *MYD88*, *ATM*, *ENDOG*, *PRKAR1B*, *BID*, and *AKT3*

NES, normalized enriched score; NOM P-value, nominal P-value; FDR P-value, false discovery rate P-value.

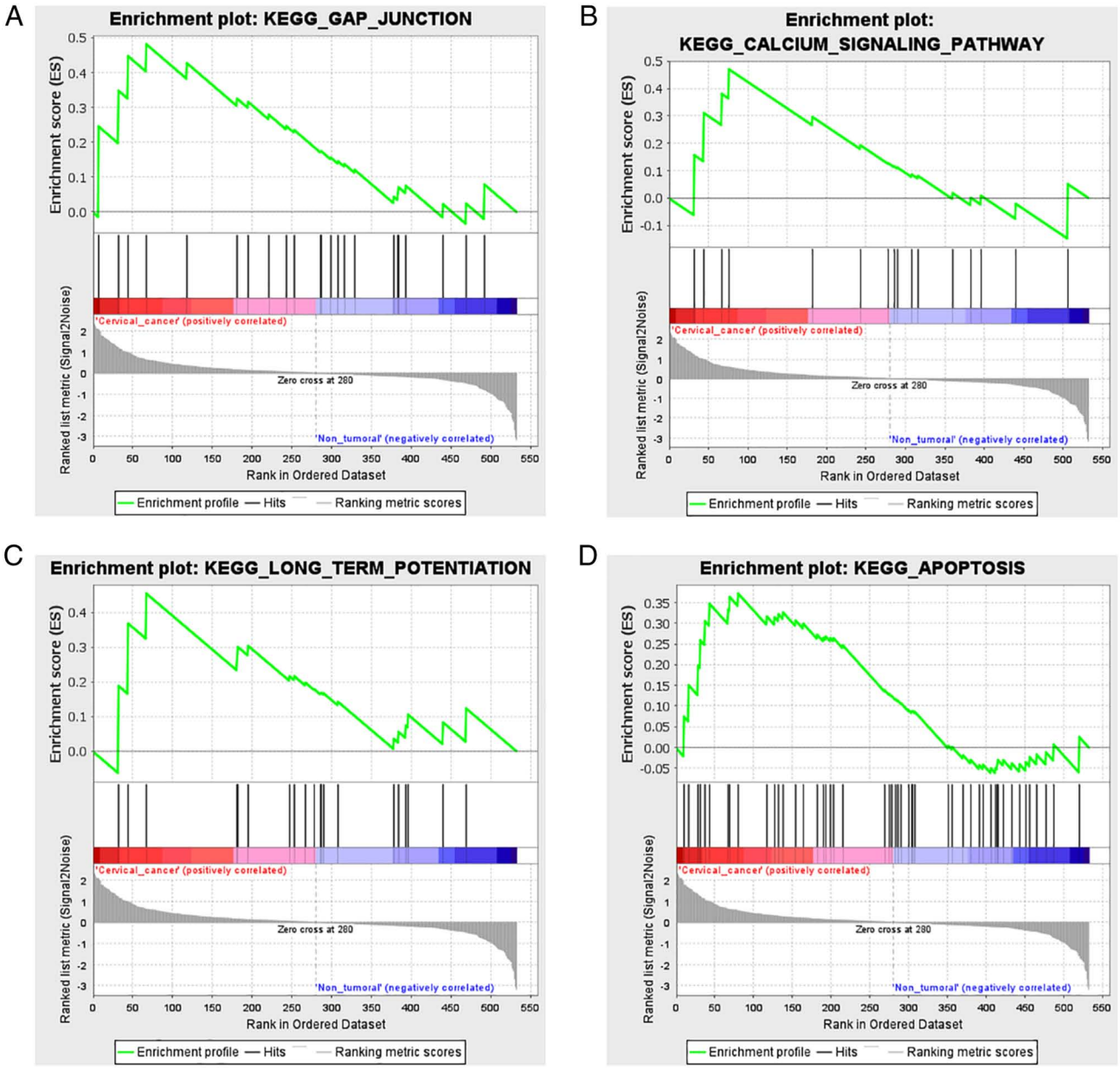

Figure 8. GSEA. GSEA was performed in the HCB-514 and HaCaT cells. The GSEA algorithm calculates an enrichment score reflecting the degree of over-representation at the top or bottom of the ranked list of the genes included in a gene set in a ranked list of all genes present in the nCounter PanCancer Pathways Panel. The analysis demonstrates that the signaling pathways (A) gap junction, (B) calcium signaling pathway, (C) long-term potentiation and (D) apoptosis were enriched in HCB-514 cells. GSEA, gene set enrichment analysis

Despite the novelty of the current findings, the present study has several limitations. First, cell proliferation was not evaluated in the HCB-514 cell line. Therefore, it should be emphasized that this analysis should be performed in the HCB-514 cell line. Although the present study evaluated the expression of DLL1 and WNT10A using *in silico* analysis, and also in the HCB-514 cell line with miR-13a-3p expression modulation, additional experiments are required to validate the possible regulatory targets of miR-130a-3p. Therefore, it would be beneficial to determine whether DLL1 and WNT10A expression are also altered in the CaSki and C-4I cell lines following miR-13a-3p inhibition. In this sense, another limitation of this study includes the absence of western blot analyses in order to validate protein expression involved in the signaling pathways identified from the pathway enrichment analysis, and also the GSEA analysis. The current analyses were performed *in vitro*; thus, future *in vivo* experiments are also warranted to further support the present conclusions. However, bearing in mind that the present study was a hypothesis-generating study, it is considered that the data identified herein are sufficiently robust and can be evaluated in a more complete manner in a future study.

In conclusion, the present study demonstrated that miR-130a-3p was highly expressed in cervical cancer cells. Cervical cancer adhesion-independent cell proliferation, migration and invasion may be suppressed by the inhibition of miR-130a-3p expression (Fig. 9). Thus, the results presented herein may provide novel insight into the role of miR-130a-3p in cervical cancer progression and its potential value for clinical prognosis.

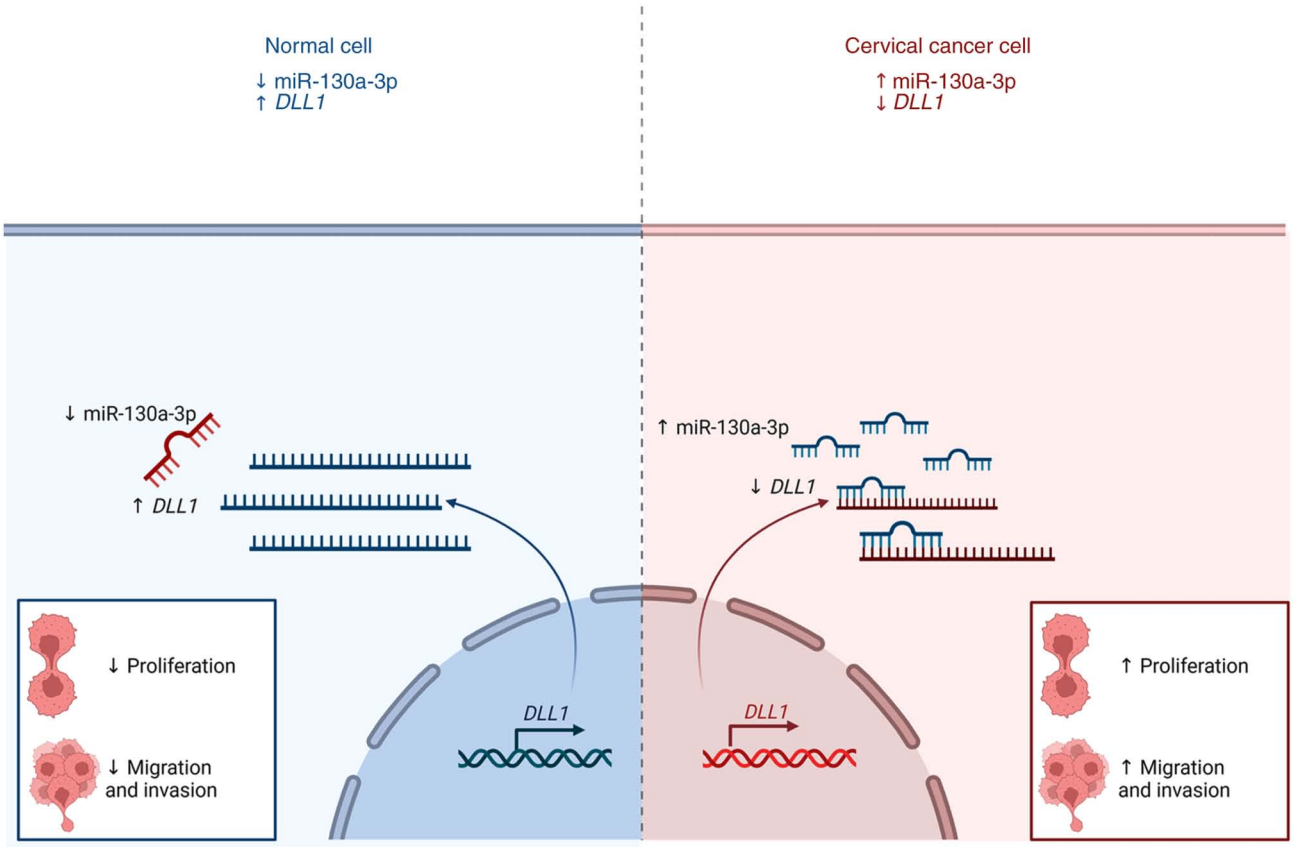

Figure 9. Graphical summary of the possible mechanism of the regulation of miR-130a-3p in cervical cancer cells. The high expression of miR-130a-3p in cervical cancer cells may promote the proliferation, migration and invasion of cervical cancer cells. By contrast, the inhibition of miR-130a-3p expression exerts opposite effects. miR, microRNA; *DLL1*, delta-like notch 1 ligand.

Acknowledgements

The authors are grateful to the researchers, Dr Laura Sicherond Dr Luisa Lina Villa (Center for Translational Investigation in Oncology, Instituto do Cancer do Estado de Sao Paulo, Hospital das Clinicas da Faculdade de Medicina da Universidade de São Paulo, São Paulo, Brazil), for kindly providing the HaCaT cell line for the initial testing in the present study.

Funding

The present study was funded by FAPESP (grant no. 2016/15831-3), the Research Incentive Program of Barretos Cancer Hospital (PAIP) and PRONON. The present study was also funded by the São Paulo Research Foundation (FAPESP; grant no. 2018/19476-9) and this research was funded by the Brazilian Ministry of Health supported by PRONON/MS (NUP-25000.023997.2018/34) entitled: 'Identificação de biomarcadores para screening e detecção precoce de tumores no contexto do Sistema Único de Saúde (SUS).' RMR and MMCM are recipients of a CNPq Productivity fellowship.

Availability of data and materials

Data regarding gene expression analysis are available on the National Center for Biotechnology Information (NCBI)-Gene Expression Omnibus (GEO) platform (https://www.ncbi.nlm.nih.gov/geo/query/acc.cgi) under the Accession no. GSE224301. The other datasets used and/or analyzed during the current study are available from the corresponding author on reasonable request.

Authors' contributions

RLC developed and led the overall study, conducted the data reviews and the analysis, and was involved in the preparation of the draft. AVHL participated in the design of the study, in functional assays and in developing the study, as well as in the critical reviewing of the manuscript. INFG participated in the conception and design of the study, as well as in the critical reviewing of the manuscript. AJADF participated in the functional assays, and in the critical reviewing of the manuscript. MNR participated in the conception and design of the study, as well as in the critical reviewing of the manuscript. RDR participated in designing and developing the study, and in the critical reading of the manuscript. RMR participated in designing and developing the study, as well as in funding, and the critical reading of the manuscript. MMCM conceived the study, provided advice during the study's development, and participated in the preparation the manuscript. RLC and MMCM confirm the authenticity of all the raw data. All authors have read and approved the final manuscript.

Ethics approval and consent to participate

Not applicable.

Patient consent for publication

Not applicable.

Competing interests

The authors declare that they have not competing interests.

References

1. Sung H, Ferlay J, Siegel RL, Laversanne M, Soerjomataram I, Jemal A and Bray F: Global cancer statistics 2020: GLOBOCAN estimates of incidence and mortality worldwide for 36 cancers in 185 countries. CA Cancer J Clin 71: 209-249, 2021.
2. Espenel S, Garcia MA, Trone JC, Guillaume E, Harris A, Rehailia-Blanchard A, He MY, Ouni S, Vallard A, Rancoule C, *et al*: From IB2 to IIIB locally advanced cervical cancers: report of a ten-year experience. Radiat Oncol 13: 16, 2018.
3. Robin TP, Amini A, Schefter TE, Behbakht K and Fisher CM: Disparities in standard of care treatment and associated survival decrement in patients with locally advanced cervical cancer. Gynecol Oncol 143: 319-325, 2016.
4. Koh WJ, Abu-Rustum NR, Bean S, Bradley K, Campos SM, Cho KR, Chon HS, Chu C, Clark R, Cohn D, *et al*: Cervical cancer, Version 3.2019, NCCN clinical practice guidelines in oncology. J Natl Compr Canc Netw 17: 64-84, 2019.
5. He Y, Han SB, Liu Y, Zhang JJ and Wu YM: Role of APOA1 in the resistance to platinum-based chemotherapy in squamous cervical cancer. BMC Cancer 22: 411, 2022.
6. International Agency for Research on Cancer I, organizador. IARC monographs on the evaluation of carcinogenic risks to humans. Vol 90. Human papillomaviruses: This publication represents the views and expert opinions of an IARC Working Group on the Evaluation of Carcinogenic Risks to Humans which met in Lyon, 15-22 February 2005. IARC, Lyon, pp670, 2007.
7. Da Silva MLR, De Albuquerque BHDR, Allyrio TADMF, De Almeida VD, Cobucci RNDO, Bezerra FL, Andrade VS, Lanza DCF, De Azevedo JCV, De Araújo JMG and Fernandes JV: The role of HPV-induced epigenetic changes in cervical carcinogenesis (Review). Biomed Rep 15: 60, 2021.
8. Hanahan D: Hallmarks of Cancer: New dimensions. Cancer Discov 12: 31-46, 2022.
9. Wang J and Chen L: The role of miRNAs in the invasion and metastasis of cervical cancer. Biosci Rep 39: BSR20181377, 2019.
10. Gao C, Zhou C, Zhuang J, Liu L, Liu C, Li H, Liu G, Wei J and Sun C: MicroRNA expression in cervical cancer: Novel diagnostic and prognostic biomarkers. J Cell Biochem 119: 7080-7090, 2018.
11. Siomi H and Siomi MC: Posttranscriptional regulation of microRNA biogenesis in animals. Mol Cell 38: 323-332, 2010.
12. Ardekani AM and Naeini MM: The Role of MicroRNAs in human diseases. Avicenna J Med Biotechnol 2: 161-179, 2010.
13. Causin RL, Freitas AJA de, Trovo Hidalgo Filho CM, Reis R dos, Reis RM and Marques MMC: A systematic review of MicroRNAs involved in cervical cancer progression. Cells 10: 668, 2021.
14. Kovall RA, Gebelein B, Sprinzak D and Kopan R: The canonical notch signaling pathway: Structural and biochemical insights into shape, sugar, and force. Dev Cell 41: 228-241, 2017.
15. Bray SJ: Notch signalling in context. Nat Rev Mol Cell Biol 17: 722-735, 2016.
16. Penton AL, Leonard LD and Spinner NB: Notch signaling in human development and disease. Semin Cell Dev Biol 23: 450-457, 2012.
17. Capaccione KM and Pine SR: The Notch signaling pathway as a mediator of tumor survival. Carcinogenesis 34: 1420-1430, 2013.
18. Briot A and Iruela-Arispe ML: Blockade of specific NOTCH ligands: A new promising approach in cancer therapy. Cancer Discov 5: 112-114, 2015.
19. Khelil M, Griffin H, Bleeker MCG, Steenbergen RDM, Zheng K, Saunders-Wood T, Samuels S, Rotman J, Vos W, van den Akker BE, *et al*: Delta-like ligand-notch1 signaling is selectively modulated by HPV16 E6 to promote squamous cell proliferation and correlates with cervical cancer prognosis. Cancer Res 81: 1909-1921, 2021.
20. Causin RL, da Silva LS, Evangelista AF, Leal LF, Souza KCB, Pessôa-Pereira D, Matsushita GM, Reis RM, Fregnani JHTG and Marques MMC: MicroRNA biomarkers of high-grade cervical intraepithelial neoplasia in liquid biopsy. Biomed Res Int 2021: 6650966, 2021.
21. He L, Wang HY, Zhang L, Huang L, Li JD, Xiong Y, Zhang MY, Jia WH, Yun JP, Luo RZ and Zheng M: Prognostic significance of low DICER expression regulated by miR-130a in cervical cancer. Cell Death Dis 5: e1205-e1205, 2014.
22. Fan Q, Huang T, Sun X, Yang X, Wang J, Liu Y, Ni T, Gu S, Li Y and Wang Y: miR-130a-3p promotes cell proliferation and invasion by targeting estrogen receptor α and androgen receptor in cervical cancer. Exp Ther Med 21: 414, 2021.
23. Rosa MN, Evangelista AF, Leal LF, De Oliveira CM, Silva VAO, Munari CC, Munari FF, Matsushita GM, Dos Reis R, Andrade CE, *et al*: Establishment, molecular and biological characterization of HCB-514: A novel human cervical cancer cell line. Sci Rep 9: 1913, 2019.
24. Silva-Oliveira RJ, Silva VAO, Martinho O, Cruvinel-Carloni A, Melendez ME, Rosa MN, de Paula FE, de Souza Viana L, Carvalho AL and Reis RM: Cytotoxicity of allitinib, an irreversible anti-EGFR agent, in a large panel of human cancer-derived cell lines: KRAS mutation status as a predictive biomarker. Cell Oncol (Dordr) 39: 253-263, 2016.
25. miRCURY LNA miRNA Inhibitors and Power Inhibitors. [Citado 9 de fevereiro de 2023]. Disponível em: https://www.qiagen.com/us/products/discovery-and-translational-research/functional-and-cell-analysis/mirna-functional-anal-sis/mircury-lna-mirna-inhibitors/mircury-lna-mirna-inhibitors?catno=339126.
26. Livak KJ and Schmittgen TD: Analysis of relative gene expression data using real-time quantitative PCR and the 2(-Delta Delta C(T)) method. Methods 25: 402-408, 2001.
27. Schmittgen TD and Livak KJ. Analyzing real-time PCR data by the comparative C(T) method. Nat Protoc 3: 1101-1108, 2008.
28. Causin RL, Pessôa-Pereira D, Souza KCB, Evangelista AF, Reis RMV, Fregnani JHTG and Marques MMC: Identification and performance evaluation of housekeeping genes for microRNA expression normalization by reverse transcription-quantitative PCR using liquid-based cervical cytology samples. Oncol Lett 18: 4753-4761, 2019.
29. Geissmann Q: OpenCFU, a new free and open-source software to count cell colonies and other circular objects. PLoS One 8: e54072, 2013.
30. Hu Y, Sun X, Mao C, Guo G, Ye S, Xu J, Zou R, Chen J, Wang L, Duan P and Xue X: Upregulation of long noncoding RNA TUG1 promotes cervical cancer cell proliferation and migration. Cancer Med 6: 471-482, 2017.
31. Yew TL, Hung YT, Li HY, Chen HW, Chen LL, Tsai KS, Chiou SH, Chao KC, Huang TF, Chen HL and Hung SC: Enhancement of wound healing by human multipotent stromal cell conditioned medium: The paracrine factors and p38 MAPK activation. Cell Transplant 20: 693-706, 2011.
32. Martinho O, Silva-Oliveira R, Miranda-Gonçalves V, Clara C, Almeida JR, Carvalho AL, Barata JT and Reis RM: In vitro and in vivo analysis of RTK inhibitor efficacy and identification of its novel targets in glioblastomas. Transl Oncol 6: 187-196, 2013.
33. de Andrade DAP, da Silva LS, Laus AC, de Lima MA, Berardinelli GN, da Silva VD, Matsushita GM, Bonatelli M, da Silva ALV, Evangelista AF, *et al*: A 4-Gene signature associated with recurrence in low- and intermediate-risk endometrial cancer. Front Oncol 11: 729219, 2021.
34. Tokar T, Pastrello C, Rossos AEM, Abovsky M, Hauschild AC, Tsay M, Lu R and Jurisica I: mirDIP 4.1-integrative database of human microRNA target predictions. Nucleic Acids Res 46: D360-D370, 2018.
35. Agarwal V, Bell GW, Nam JW and Bartel DP: Predicting effective microRNA target sites in mammalian mRNAs. Elife 4: e05005, 2015.
36. Shannon P, Markiel A, Ozier O, Baliga NS, Wang JT, Ramage D, Amin N, Schwikowski B and Ideker T: Cytoscape: A software environment for integrated models of biomolecular interaction networks. Genome Res 13: 2498-2504.
37. Tang Z, Kang B, Li C, Chen T and Zhang Z: GEPIA2: An enhanced web server for large-scale expression profiling and interactive analysis. Nucleic Acids Res 47: W556-W560, 2019.
38. Park SJ, Yoon BH, Kim SK and Kim SY: GENT2: An updated gene expression database for normal and tumor tissues. BMC Medical Genomics 12 (Suppl 5): S101, 2019.

39. Subramanian A, Tamayo P, Mootha VK, Mukherjee S, Ebert BL, Gillette MA, Paulovich A, Pomeroy SL, Golub TR, Lander ES and Mesirov JP: Gene set enrichment analysis: A knowledge-based approach for interpreting genome-wide expression profiles. Proc Natl Acad Sci USA 102: 15545-1550, 2005.
40. Mootha VK, Lindgren CM, Eriksson KF, Subramanian A, Sihag S, Lehar J, Puigserver P, Carlsson E, Ridderstråle M, Laurila E, *et al*: PGC-1alpha-responsive genes involved in oxidative phosphorylation are coordinately downregulated in human diabetes. Nat Genet 34: 267-273, 2003.
41. Liberzon A, Subramanian A, Pinchback R, Thorvaldsdóttir H, Tamayo P and Mesirov JP: Molecular signatures database (MSigDB) 3.0. Bioinformatics 27: 1739-1740, 2011.
42. Liberzon A, Birger C, Thorvaldsdóttir H, Ghandi M, Mesirov JP and Tamayo P: The molecular signatures database (MSigDB) hallmark gene set collection. Cell Syst 1: 417-425, 2015.
43. Zhang H da, Jiang LH, Sun DW, Li J and Ji ZL: The role of miR-130a in cancer. Breast Cancer 24: 521-527, 2017.
44. Wang M, Wang X and Liu W: MicroRNA-130a-3p promotes the proliferation and inhibits the apoptosis of cervical cancer cells via negative regulation of RUNX3. Mol Med Rep 22: 2990-3000, 2020.
45. Zhao X, Jin X, Zhang Q, Liu R, Luo H, Yang Z, Geng Y, Feng S, Li C, Wang L, *et al*: Silencing of the lncRNA H19 enhances sensitivity to X-ray and carbon-ions through the miR-130a-3p /WNK3 signaling axis in NSCLC cells. Cancer Cell Int 21: 644, 2021.
46. Hu W, Zheng X, Liu J, Zhang M, Liang Y and Song M: MicroRNA MiR-130a-3p promotes gastric cancer by targeting Glucosaminyl N-acetyl transferase 4 (GCNT4) to regulate the TGF-β1/SMAD3 pathway. Bioengineered 12: 11634-1147, 2021.
47. Huang J, Zhao M, Hu H, Wang J, Ang L and Zheng L. MicroRNA-130a reduces drug resistance in breast cancer. Int J Clin Exp Pathol 12: 2699-2705, 2019.
48. Liu Y, Li Y, Wang R, Qin S, Liu J, Su F, Yang Y, Zhao F, Wang Z and Wu Q: MiR-130a-3p regulates cell migration and invasion via inhibition of Smad4 in gemcitabine resistant hepatoma cells. J Exp Clin Cancer Res 35: 19, 2016.
49. Yu F, Fan X, Chen B, Dong P and Zheng J: Activation of hepatic stellate cells is inhibited by microRNA-378a-3p via Wnt10a. Cell Physiol Biochem 39: 2409-2420, 2016.
50. Zhou H, Tang H, Li N, Chen H, Chen X, Gu L, Zhang L, Tian G and Tao D: MicroRNA-361-3p inhibit the progression of lymphoma by the Wnt/β-catenin signaling pathway. Cancer Manag Res 12: 12375-12384, .2020